

Title: Old carbon reservoirs were not important in the deglacial methane budget

Authors: M.N. Dyonisius^{1*}, V.V. Petrenko¹, A.M. Smith², Q. Hua², B. Yang², J. Schmitt³, J. Beck³, B. Seth³, M. Bock³, B. Hmiel¹, I. Vimont^{4,†}, J.A. Menking⁵, S.A. Shackleton^{6,‡}, D. Baggenstos^{6,3}, T.K. Bauska^{5,7}, R.H. Rhodes^{5,8}, P. Sperlich⁹, R. Beaudette⁶, C. Harth⁶, M. Kalk⁵, E.J. Brook⁵, H. Fischer³, J.P. Severinghaus⁶, R.F. Weiss⁶

Affiliations:

¹Department of Earth and Environmental Sciences, University of Rochester, Rochester, NY 14627, USA

²Australian Nuclear Science and Technology Organisation (ANSTO), Lucas Heights, NSW 2234, Australia.

³Climate and Environmental Physics, Physics Institute and Oeschger Centre for Climate Change Research, University of Bern, CH-3012 Bern, Switzerland

⁴Institute of Arctic and Alpine Research, University of Colorado Boulder, Boulder, CO 80303, USA

⁵College of Earth, Ocean and Atmospheric Sciences, Oregon State University, Corvallis, OR, 97331, USA

⁶Scripps Institution of Oceanography (SIO), University of California, San Diego, La Jolla, CA 92037, USA

⁷British Antarctic Survey High Cross, Cambridge CB3 0ET, UK.

⁸Department of Earth Sciences, University of Cambridge, Cambridge CB2 3EQ, UK

⁹National Institute of Water and Atmospheric Research (NIWA), 6021 Wellington, New Zealand

* Correspondence to: mdyonisi@ur.rochester.edu

† Present address: Cooperative Institute for Research in Earth Sciences, University of Colorado, Boulder, USA

‡ Present address: Department of Geosciences, Princeton University, Princeton, NJ 08544 USA

Abstract: Permafrost and methane hydrates are large, climate-sensitive old carbon reservoirs that have the potential to emit large quantities of methane, a potent greenhouse gas, as the Earth continues to warm. We present ice core isotopic measurements of methane ($\Delta^{14}\text{C}$, $\delta^{13}\text{C}$, and δD) from the last deglaciation, which is a partial analog for modern warming. Our results show that methane emissions from old carbon reservoirs in response to deglacial warming were small (<19 teragrams of methane per year, 95% confidence interval) and argue against similar methane emissions in response to future warming. Our results also indicate that methane emissions from biomass burning in the pre-Industrial Holocene were 22–56 teragrams of methane per year (95% confidence interval), which is comparable to today.

Main Text: Methane (CH_4) is an important contributor to the greenhouse effect with a global warming potential ~28 times higher than carbon dioxide (CO_2) on a 100-year timescale (1). Natural CH_4 emissions currently account for ~40% of total emissions (2), and there are

considerable uncertainties in their response to future warming (3). Although wetlands are the dominant natural source of CH₄, increased emissions from large, climate-sensitive old carbon reservoirs such as permafrost (4) and hydrates under ice sheets (5) might become important in the coming century. Marine hydrates may also have the potential to emit substantial amount of CH₄ into the atmosphere in response to warming (6), but the timescale of marine hydrate dissociation is relatively long (on the order of hundreds to thousands of years). Furthermore, there is a growing consensus that CH₄ release to the atmosphere from dissociating marine hydrates will be buffered by efficient CH₄ oxidation in the sediments and water column (3,7).

The last deglaciation [18–8 kilo-annum before present, (ka BP)] provides the opportunity for evaluating the long-term sensitivity of these old carbon reservoirs (marine hydrates, permafrost, and hydrates under ice sheet) to a changing climate. There is abundant evidence of the destabilization of marine hydrates (8, 9), land permafrost degradation (10), and thermokarst lake (permafrost thaw lake) formation (11) during the last deglaciation. However, CH₄ emissions from these old carbon reservoirs into the atmosphere are not well constrained. The paleoatmospheric CH₄ mole fraction and its isotopic composition from trapped air in ice cores provide a historical perspective on how natural CH₄ sources respond to climate change (e.g., 12, 13). Measurements of carbon-14 (¹⁴C) of CH₄ (¹⁴CH₄) from ice cores specifically provide an unambiguous top-down constraint on the globally integrated ¹⁴C-free CH₄ emissions from all old carbon reservoirs.

¹⁴C decays radioactively and is thus strongly depleted in carbon reservoirs that have been isolated from the atmosphere for time periods longer than its half-life of ~5730 years. Because of the low abundance of ¹⁴C (on the order of 10⁻¹² compared to ¹²C), measurements of ¹⁴CH₄ in ice cores are challenging, requiring ~1000 kg of ice per sample. We collected ice cores from a well-dated ice ablation site on Taylor Glacier, Antarctica (14), which provides easy access to large volumes of old ice at shallow depths. Petrenko *et al.* (15) recently presented measurements of paleoatmospheric ¹⁴CH₄ from Taylor Glacier for the Younger Dryas-Preboreal (YD-PB) transition (11.7 to 11.3 ka BP) and concluded that ¹⁴C-free CH₄ emissions were small [$< 7.7\%$ of total CH₄ emissions, 95% confidence interval (CI)]. However, their results only spanned a brief time interval within the deglacial transition. In this study we present 11 additional measurements of paleoatmospheric ¹⁴CH₄ (Fig. 1A) combined with stable isotope measurements ($\delta^{13}\text{CH}_4$ and $\delta\text{D-CH}_4$) (Fig. 1C, 1D) in the 15 to 8 ka BP time interval, providing a more complete picture of the deglacial CH₄ budget.

The Oldest Dryas-Bølling (OD-B) transition (14.6 to 14.45 ka BP) represents the first large and abrupt CH₄ rise during the last deglacial sequence of events (Fig. 1B) at the time when sea level was ~100 m lower than today. This abrupt CH₄ rise was synchronous with the acceleration of Northern Hemisphere (NH) warming (16) (Fig. 1E), ice sheet retreat, and rapid sea level rise (17). This climate transition may have also coincided with the first instance of marine hydrate destabilization during the last deglaciation caused by hydrostatic pressure relief from NH ice sheet retreat and incursion of warm intermediate ocean water into shallow hydrate-bearing Arctic sediments (8). During the destabilization of marine hydrate reservoirs, abrupt events such as submarine landslides (18) or collapse of marine hydrate pingos (8) could result in large and rapid CH₄ expulsions that may have contributed to the rapid atmospheric CH₄ rise (9) if they were capable of bypassing oxidation in the water column.

In contrast to old carbon reservoirs, contemporaneous CH₄ sources such as wetlands and biomass burning emit CH₄ with a ¹⁴C signature that reflects the contemporaneous $\Delta^{14}\text{CO}_2$ at the

time (15). Our $\Delta^{14}\text{CH}_4$ measurements for the OD-B transition are all within 1σ uncertainty of the contemporaneous atmospheric $\Delta^{14}\text{CO}_2$ (19) (Fig. 1A) – indicating a dominant role of contemporaneous CH_4 sources. We used a one-box model (see section 4.2 of the materials and methods) (20) to calculate the amount of ^{14}C -free CH_4 emissions to the atmosphere (Table 1, fig. S9, and table S10) (20). Our box model shows that the total ^{14}C -free CH_4 emissions during the OD-B transition were small [on average, <13 teragrams (Tg) of CH_4 per year, Tg CH_4/yr , 95% CI upper limit]. Combined with earlier $\Delta^{14}\text{CH}_4$ data from the YD-PB transition (15), our results argue strongly against the hypothesis regarding old carbon reservoirs being important contributors to the rapid CH_4 increases associated with abrupt warming events (Dansgaard-Oeschger events) (9). This conclusion is consistent with previous studies (13) that show no major enrichment in the CH_4 deuterium / hydrogen ratio ($\delta\text{D-CH}_4$) concurrent with the abrupt CH_4 transitions (CH_4 from marine hydrates is relatively enriched in δD). It has been shown that even at a relatively shallow water depth of ~30 m, ~90% of the ^{14}C -free CH_4 released from thawing subsea permafrost was oxidized in the water column (21). We hypothesize that during the OD-B transition, relatively rapid sea level rise associated with meltwater pulse (MWP) 1-A (17), combined with CH_4 oxidation in the water column (22) may have prevented CH_4 emissions from disintegrating marine hydrates and subsea permafrost from reaching the atmosphere.

Our measurements of $^{14}\text{CH}_4$ during the Bølling-Allerød interstadial (14.45 to 13 ka BP) and the early Holocene (10 to 8 ka BP) warm period (Fig. 1A) provide an opportunity to assess the likelihood of delayed CH_4 emissions from old carbon reservoirs in response to warming. The onset of marine hydrate dissociation might lag the initial warming signal on decadal (23), centennial, or even millennial (18) time scales. Permafrost degradation could also lag a warming signal on decadal and centennial timescales (24) depending on local environmental conditions such as permafrost depth, soil types, and moisture content (4). During parts of the early Holocene, Arctic temperatures were likely warmer than today (25), providing a good analog for Arctic conditions in the coming decades. Proxy reconstructions of thermokarst lake initiation (11) and land permafrost degradation (10, 24) suggested a potential increase of CH_4 emissions from these processes during both the Bølling-Allerød interstadial and early Holocene warm period. However, our $\Delta^{14}\text{CH}_4$ measurements (Fig. 1A and Table 1) show no evidence of delayed ^{14}C -free CH_4 emissions following warming. These results are consistent with present-day observations that carbon from thermokarst lakes and permafrost is predominantly emitted in the form of CO_2 rather than CH_4 (4, 26), and that CH_4 emissions from permafrost systems are dominated by relatively contemporaneous carbon (26, 27).

Because carbon stored in permafrost is not expected to be ^{14}C -free (28), we also attempted to use our $^{14}\text{CH}_4$ results to calculate the possible magnitude of CH_4 emissions from thawing old carbon in permafrost (Section 4.3) (20). This calculation assumed that ^{14}C activity of permafrost CH_4 emissions follows the predepositional age of terrigenous biomarkers released from thawing permafrost (7500 ± 2500 yrs old relative to our sample age) (10). Resulting CH_4 emissions from old permafrost carbon range from 0 to 53 Tg CH_4/yr (table S10) (20) throughout the last deglaciation and may have contributed up to 27% of the total CH_4 emissions to the atmosphere (95% CI upper limit) at the end of the OD-B transition (14.42 ka BP). However, we consider this calculation speculative (see section 4.3 of the materials and methods) (20).

When the global sea level was lower, exposure of continental shelves may have resulted in higher CH_4 emissions from natural geologic seeps (29). A recent study also inferred the

existence of methane hydrate deposits underneath ice sheets and suggested that the proglacial meltwater discharge is likely an important source of CH₄ to the atmosphere (5). Ice sheet retreat during the last deglaciation may have destabilized the subglacial hydrate deposits, which contain old, ¹⁴C-depleted CH₄. However, our data, which span most of the deglacial ice retreat and sea level rise (Fig. 1F) argue strongly against both hypotheses. The ¹⁴C-free CH₄ emissions were small throughout the last deglaciation (Table 1) and appear to be insensitive to both global sea level and ice volume.

Biomass burning is an important component of the global carbon cycle and is tightly coupled with emissions of carbon monoxide (CO), nitrogen oxides (NO_x), non-methane hydrocarbons (NMHC), and aerosols that have substantial effects on atmospheric chemistry and radiative energy fluxes. Compared with other proxies of past biomass burning, CH₄ has an advantage because it is a well-mixed gas in the atmosphere and can represent the globally integrated biomass-burning emissions. Bock *et al.* (13) provided the most recent stable isotope-based ($\delta^{13}\text{C}$ and δD) study of the glacial-interglacial CH₄ budget, but they were unable to separate the relative contributions from CH₄ sources that are enriched in heavier isotopes (biomass burning and natural geologic emissions). With improved estimates of natural geologic emissions, our results allow for better constraints on the overall CH₄ budget. We used the stable isotope data (Fig. 1C, Fig. 1D) in a one-box model (see section 5 of the materials and methods) (20) to calculate CH₄ emissions from biomass burning (CH₄_{bb}) and microbial sources (CH₄_{mic}, composed of emissions from wetlands, ruminants, and termites) for the Early Holocene (Table 1, fig. S11) (20). We extended our calculation to the late Holocene (~2 ka BP) (Table 1) to directly compare our CH₄ source strength estimates to those of earlier studies (30, 31). This assumption can be justified because a large change in the natural geologic emissions between the early Holocene and 2 ka BP seems unlikely, as global sea level and ice volume did not change appreciably after 8 ka BP (32). However, we did not perform this calculation for the pre-Holocene samples because estimates of the CH₄ inter-polar difference, atmospheric global-average CH₄ stable isotope values, and stable isotopic signatures of the sources are more uncertain (Section 5) (20).

We calculated relatively high CH₄_{bb} emissions in the early Holocene (33 to 56 Tg CH₄/yr, 95% CI) at 10 ka BP and a slight decrease of CH₄_{bb} emissions (22 to 42 Tg CH₄/yr, 95% CI) towards the late Holocene (Table 1). However, we note that the magnitude of the decrease in biomass burning emissions (~7 Tg CH₄/yr) is small relative to the uncertainties for both the CH₄_{bb} and CH₄_{mic} emissions (± 11 Tg CH₄/yr and ± 18 Tg CH₄/yr respectively, 95% CI uncertainties). Our estimate of 22 to 42 Tg CH₄/yr (95% CI) CH₄_{bb} emissions for the late Holocene period (~2 ka BP) is within the upper range of estimates from prior ice core studies (13, 30, 31). Considering the large downward revision of natural geologic emissions inferred from our ¹⁴C data, an upward revision in pyrogenic CH₄ emissions is expected to balance the CH₄ stable isotope budget. The increase in CH₄_{bb} expected from a reduction in natural geologic emissions is partly offset by a -0.5 to -1‰ revision in atmospheric $\delta^{13}\text{C}$ values (12, 30, 31) because the $\delta^{13}\text{C}$ values from earlier studies (30, 31) were likely biased due to krypton (Kr) interference (33). Our CH₄_{bb} estimates are also reduced because, unlike prior studies, we accounted for temporal shifts in the isotopic signatures of CH₄_{bb} and CH₄_{mic} between the pre-Industrial Holocene and the modern period expected from anthropogenically-driven changes in the $\delta^{13}\text{C}$ CO₂ precursor material and land use (see section 5.2 of materials and methods) (20). Our best CH₄_{bb} estimates for the late Holocene (22 to 42 Tg CH₄/yr, 95% CI) are comparable to the present-day estimates of combined pyrogenic CH₄ emissions from anthropogenic biomass burning and

wildfires (2). This result is supported by some (34, 35), but not all (36) independent paleoproxies of biomass burning.

The last deglaciation serves only as a partial analog to current anthropogenic warming, with the most significant differences being the much colder baseline temperature, lower sea level, and the presence of large ice sheets covering a large part of what are currently permafrost regions in the NH. Although Arctic temperatures during the peak early Holocene warmth were likely warmer than today (25), they were still lower than the Arctic temperature projections by the end of this century under most warming scenarios (37). However, there are also many similarities between the last deglaciation and current anthropogenic warming. Both deglacial and modern warming include strong Arctic amplification, and the magnitude of global warming (~4°C) (16) during the last deglaciation was comparable to the expected magnitude of equilibrium global temperature change under mid-range anthropogenic emission scenarios (37). Because the relatively large global warming of the last deglaciation (which included periods of large and rapid regional warming in the high latitudes) did not trigger CH₄ emissions from old carbon reservoirs, such CH₄ emissions in response to anthropogenic warming also appear to be unlikely. Our results instead support the hypothesis that natural CH₄ emissions involving contemporaneous carbon from wetlands are likely to increase as warming continues (38). We also estimated relatively high CH₄_{bb} emissions for the pre-Industrial Holocene that were comparable to present-day combined pyrogenic CH₄ emissions from natural and anthropogenic sources. This result suggests either an underestimation of present-day CH₄_{bb} or a two-way anthropogenic influence on fire activity during the Industrial Revolution: reduction in wildfires from active fire suppression and landscape fragmentation balanced by increased fire emissions from land-use change (deforestation) and traditional biofuel use (burning of plant materials for cooking and heating).

References and Notes:

1. G. Myhre, et al., in *Climate Change 2013: The Physical Science Basis. Contribution of Working Group I to the Fifth Assessment Report of the Intergovernmental Panel on Climate Change*, T. F. Stocker, et al., Eds. (Cambridge University Press, Cambridge, United Kingdom and New York, NY, USA, 2013; www.climatechange2013.org), pp. 659–740.
2. M. Saunois, et al., The global methane budget 2000-2012. *Earth. Syst. Sci. Data.* **8**, 697 (2016).
3. J. F. Dean, et al., Methane Feedbacks to the Global Climate System in a Warmer World. *Rev. Geophys.* **56**, 207–250 (2018).
4. E. A. G. Schuur, et al., Climate change and the permafrost carbon feedback. *Nature.* **520**, 171–179 (2015).
5. G. Lamarche-Gagnon, et al., Greenland melt drives continuous export of methane from the ice-sheet bed. *Nature.* **565**, 73 (2019).

6. M. Maslin, et al., Gas hydrates: past and future geohazard? *Philosophical Transactions of the Royal Society of London A: Mathematical, Physical and Engineering Sciences*. **368**, 2369–2393 (2010).
7. C. D. Ruppel, J. D. Kessler, The interaction of climate change and methane hydrates. *Rev. Geophys.*, 2016RG000534 (2017).
8. K. Andreassen, et al., Massive blow-out craters formed by hydrate-controlled methane expulsion from the Arctic seafloor. *Science*. **356**, 948–953 (2017).
9. J. P. Kennett, K. G. Cannariato, I. L. Hendy, R. J. Behl, in *Methane Hydrates in Quaternary Climate Change: The Clathrate Gun Hypothesis* (American Geophysical Union (AGU), 2013);
10. M. Winterfeld, et al., Deglacial mobilization of pre-aged terrestrial carbon from degrading permafrost. *Nat Commun*. **9**, 3666 (2018).
11. K. M. Walter, M. E. Edwards, G. Grosse, S. A. Zimov, F. S. Chapin, Thermokarst Lakes as a Source of Atmospheric CH₄ During the Last Deglaciation. *Science*. **318**, 633–636 (2007).
12. J. Beck, et al., Bipolar carbon and hydrogen isotope constraints on the Holocene methane budget. *Biogeosciences*. **15**, 7155–7175 (2018).
13. M. Bock, et al. Glacial/interglacial wetland, biomass burning, and geologic methane emissions constrained by dual stable isotopic CH₄ ice core records. *Proc. Natl. Acad. Sci.*, 201613883 (2017).
14. D. Baggenstos, et al., Atmospheric gas records from Taylor Glacier, Antarctica, reveal ancient ice with ages spanning the entire last glacial cycle. *Clim. Past*. **13**, 943 (2017).
15. V. V. Petrenko, et al., Minimal geological methane emissions during the Younger Dryas–Preboreal abrupt warming event. *Nature*. **548**, 443–446 (2017).
16. J. D. Shakun, et al., Global warming preceded by increasing carbon dioxide concentrations during the last deglaciation. *Nature*. **484**, 49–54 (2012).
17. P. Deschamps, et al., Ice-sheet collapse and sea-level rise at the Bølling warming 14,600 years ago. *Nature*. **483**, 559–564 (2012).
18. D. Archer, Methane hydrate stability and anthropogenic climate change. *Biogeosciences*. **4**, 993–1057 (2007).
19. P. J. Reimer, et al., IntCal13 and Marine13 Radiocarbon Age Calibration Curves 0–50,000 Years cal BP. *Radiocarbon*. **55**, 1869–1887 (2013).
20. see Materials and Methods

21. K. J. Sparrow, et al., Limited contribution of ancient methane to surface waters of the U.S. Beaufort Sea shelf. *Science Advances*. **4**, eaao4842 (2018).
22. M. Leonte, et al., Rapid rates of aerobic methane oxidation at the feather edge of gas hydrate stability in the waters of Hudson Canyon, US Atlantic Margin. *Geochim. Cosmochim. Acta*. **204**, 375–387 (2017).
23. Stranne C., O'Regan M., Jakobsson M., Overestimating climate warming-induced methane gas escape from the seafloor by neglecting multiphase flow dynamics. *Geophys. Res. Lett.* **43**, 8703–8712 (2016).
24. A. V. Reyes, C. A. Cooke, Northern peatland initiation lagged abrupt increases in deglacial atmospheric CH₄. *Proc. Natl. Acad. Sci.* **108**, 4748–4753 (2011).
25. B. S. Lecavalier, et al., High Arctic Holocene temperature record from the Agassiz ice cap and Greenland ice sheet evolution. *Proc. Natl. Acad. Sci.* **114**, 5952–5957 (2017).
26. C. D. Elder, et al., Greenhouse gas emissions from diverse Arctic Alaskan lakes are dominated by young carbon. *Nat. Clim. Change*. **8**, 166–171 (2018).
27. M. D. A. Cooper, et al., Limited contribution of permafrost carbon to methane release from thawing peatlands. *Nat. Clim. Change*. **7**, 507–511 (2017).
28. P. J. Mann, et al., Utilization of ancient permafrost carbon in headwaters of Arctic fluvial networks. *Nat Commun.* **6**, 7856 (2015).
29. B. Luyendyk, J. Kennett, J. F. Clark, Hypothesis for increased atmospheric methane input from hydrocarbon seeps on exposed continental shelves during glacial low sea level. *Mar. Petrol. Geol.* **22**, 591–596 (2005).
30. D. F. Ferretti, et al., Unexpected Changes to the Global Methane Budget over the Past 2000 Years. *Science*. **309**, 1714–1717 (2005).
31. C. J. Sapart, et al., Natural and anthropogenic variations in methane sources during the past two millennia. *Nature*. **490**, 85 (2012).
32. K. Lambeck, H. Rouby, A. Purcell, Y. Sun, M. Sambridge, Sea level and global ice volumes from the Last Glacial Maximum to the Holocene. *Proc. Natl. Acad. Sci.* **111**, 15296–15303 (2014).
33. J. Schmitt, et al., On the interference of Kr during carbon isotope analysis of methane using continuous-flow combustion–isotope ratio mass spectrometry. *Atmos. Meas. Tech.* **6**, 1425–1445 (2013).
34. M. R. Nicewonger, M. Aydin, M. J. Prather, E. S. Saltzman, Large changes in biomass burning over the last millennium inferred from paleoatmospheric ethane in polar ice cores. *Proc. Natl. Acad. Sci.* **115**, 12413–12418 (2018).

35. Z. Wang, J. Chappellaz, K. Park, J. E. Mak, Large Variations in Southern Hemisphere Biomass Burning During the Last 650 Years. *Science*. **330**, 1663–1666 (2010).
36. Daniau A.-L., Bartlein P. J., et al., Predictability of biomass burning in response to climate changes. *Global Biogeochem. Cy.* **26** (2012), doi:10.1029/2011GB004249.
37. M. Collins, et al., in *Climate Change 2013: The Physical Science Basis. Contribution of Working Group I to the Fifth Assessment Report of the Intergovernmental Panel on Climate Change*, T. F. Stocker, et al., Eds. (Cambridge University Press, Cambridge, United Kingdom and New York, NY, USA, 2013; www.climatechange2013.org), pp. 1029–1136.
38. P. U. Clark, A. J. Weaver, E. Brook, E. R. Cook, T. L. Delworth, K. Steffen, Abrupt Climate Change. A report by the US Climate Change Science Program and the Subcommittee on Global Change Research. *US Geological Survey, Reston, VA* (2008).
39. WAIS Divide Project Members, Precise inter-polar phasing of abrupt climate change during the last ice age. *Nature*. **520**, 661–665 (2015).
40. M. Sigl, et al., The WAIS Divide deep ice core WD2014 chronology – Part 2: Annual-layer counting (0–31 ka BP). *Clim. Past*. **12**, 769–786 (2016).

Acknowledgments: We thank M. Jayred and J. Jetson for ice drilling, camp managers K. Schroeder and C. Llewelyn, field team members A. Palardy and J. Ward for assistance; the U.S. Antarctic Program for logistical support; M. Sigl and F. Adolphi for assistance with age-scale transfer between IntCal13 and WD2014; H. Schaefer for suggestions regarding the isotope box model; G. Mollenhauer for discussions regarding the ^{14}C -age of terrigenous biomarkers; P.F. Place Jr., M. Diaz, and M. Paccico for help with field gear preparations. **Funding:** This work was supported by US NSF awards PLR-1245659 (V.V.P.), PLR- 1245821 (E.J.B.), PLR-1246148 (J.P.S.), Packard Fellowship for Science and Engineering (V.V.P.); the European Research Council (ERC) under the European Union’s Seventh Framework Programme FP7/2007-2013 ERC Grant 226172 [ERC Advanced Grant Modern Approaches to Temperature Reconstructions in Polar Ice Cores (MATRICs); H.F.] and the Swiss National Science Foundation (H.F.); Australian Government for the Centre for Accelerator Science at ANSTO through the National Collaborative Research Infrastructure Strategy (A.M.S., Q.H., B.Y.); and the National Institute of Water and Atmospheric Research through the Greenhouse Gases, Emissions and Carbon Cycle Science Program (P.S.). **Author contributions:** VVP, EJB and JPS designed the study. MND, VVP and BH conducted field logistical preparations. MND, VVP, JAM, SAS, BH, IV, DB, TKB, PS, EJB, JPS and RHR conducted the field sampling and reconnaissance. MND extracted CH_4 and CO from air samples. QH and BY graphitized the ^{14}C samples. AMS conducted the ^{14}C measurements. JB and BS made the CH_4 stable isotopes measurements ($\delta^{13}\text{C}$ and $\delta\text{D-CH}_4$) under supervision from JS, MB and HF. DB and JPS made the Xe/Kr , Kr/N_2 and Xe/N_2 measurements. RB made the $\delta^{15}\text{N}_2$, $\delta^{18}\text{O}_{\text{atm}}$, $^{40}\text{Ar}/^{36}\text{Ar}$, O_2/N_2 and Ar/N_2 measurements. CH made the CH_4 mole fraction and halogenated trace gas measurements under supervision of RFW. MK made the CH_4 mole fraction and total air content measurements on the ice samples under supervision of EJB. IV made the $\delta^{13}\text{CO}$ measurement for the CO dilution gas. SAS and MND developed the age-scale for the samples. MND and VVP analyzed the results and

wrote the manuscript with input from all authors. **Competing interests:** Authors declare no competing interests. **Data and materials availability:** Data from this work will be available via the USAP Data Center: <https://gcmd.nasa.gov/search/Metadata.do?entry=USAP-1245659>

Supplementary Materials:

Materials and Methods

Supplementary Text

Figures S1-S12

Tables S1-S11

References (41-97)

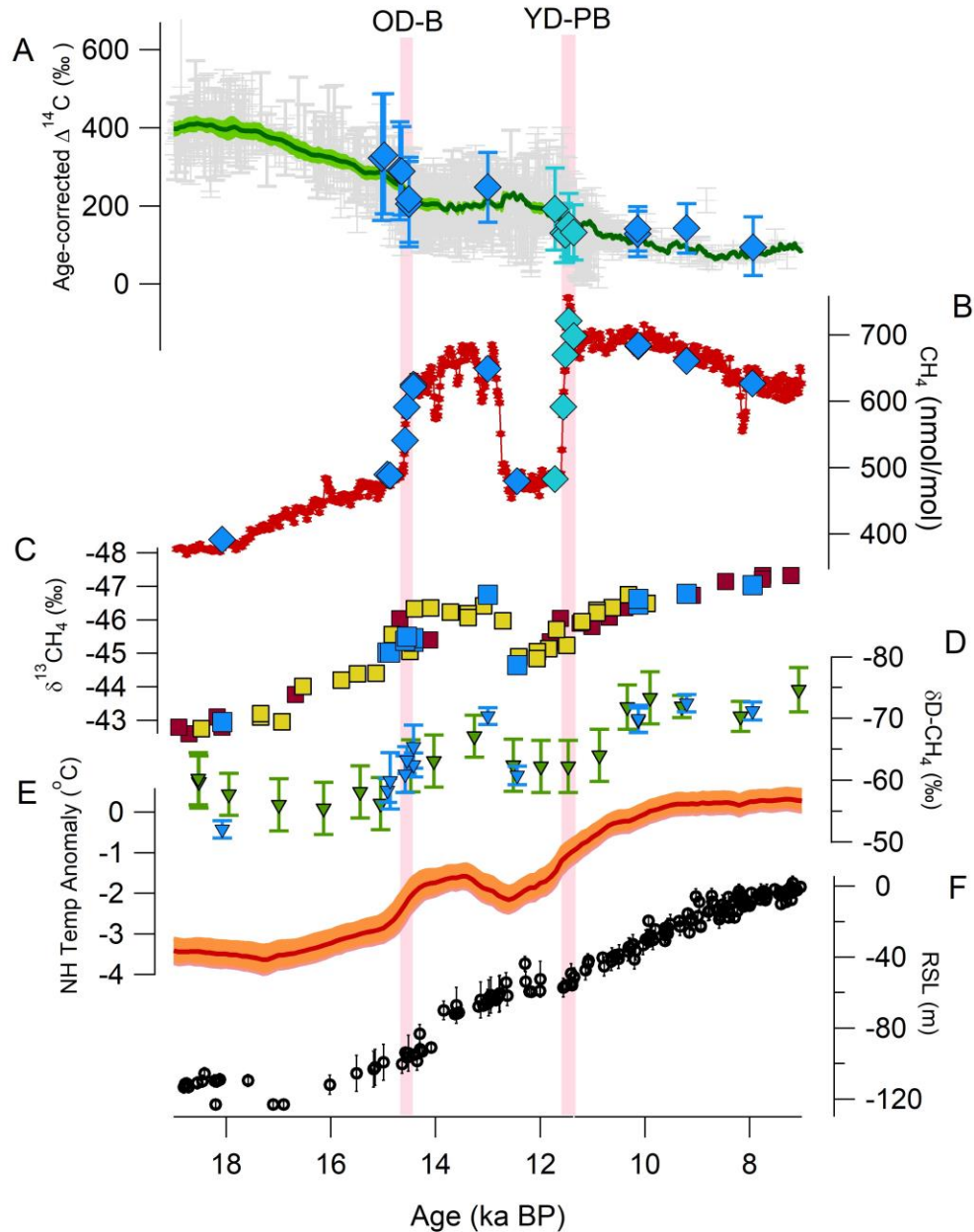


Fig. 1. CH₄ isotopes, mole fraction, NH temperature reconstruction, and relative sea level (RSL) during the last deglaciation. (A) $\Delta^{14}\text{CH}_4$ from Taylor Glacier (blue diamonds; this study), $\Delta^{14}\text{C}$ of contemporaneous CO₂ from IntCal13 [green line (19)], IntCal13 raw data [grey crosses (19)] and earlier $\Delta^{14}\text{CH}_4$ results [light blue diamonds, (15)]. Two $\Delta^{14}\text{CH}_4$ samples from the 2014/2015 field season (at 17.8 ka BP and 12.8 ka BP) were rejected because of suspected addition of extraneous ¹⁴C (see section 3 of materials and methods) (20). (B) CH₄ mole fraction from discrete WAIS Divide ice core measurements [red dots (39)], Taylor Glacier (blue diamonds; this study) and earlier Taylor Glacier study [light blue diamonds, (15)]. (C) $\delta^{13}\text{CH}_4$ from TALDICE (red squares), EDML [yellow squares, (13)] and Taylor Glacier (blue squares; this study). (D) $\delta\text{D-CH}_4$ from EDML [green triangles, (13)] and Taylor Glacier (blue triangles; this study). (E) Composite NH temperature stack (red line) and its 95% CI [shaded orange area, (16)]. (F) Global RSL inferred from coral data (32). All ice core data are plotted with respect to the WD2014 age-scale (40); IntCal13, RSL, and NH temperature stack are plotted on their respective age-scales. All error bars represent the 95% CI.

Table 1. CH₄ source strength estimates (95% CI) for time intervals of our samples. Sample ages were determined via value matching of globally well-mixed gases (CH₄ and δ¹⁸O of atmospheric oxygen) to WD2014 chronology (see section 1 of the materials and methods) (20). The sample ages given in this table represent the “best” (maximum probability) age on the probability distribution (fig. S3) (20) with respect to WD2014 chronology (40).

Sample name	Sample age (ka BP)	CH ₄ mole fraction (nmol/mol)	Age-corrected Δ ¹⁴ CH ₄ (‰)	Total source (Tg CH ₄ /yr)	¹⁴ C-free emissions (Tg CH ₄ /yr)	Biomass burning emissions (Tg CH ₄ /yr)	Microbial emissions (Tg CH ₄ /yr)
Oldest Dryas 1	14.92	484.5 ± 3.9	317 ± 166	141.3 ± 14.4	0-13	—	—
Oldest Dryas 2	14.86	485.9 ± 3.9	327 ± 151	142.3 ± 14.7	0-10	—	—
Transition 1	14.58	543.0 ± 3.9	288 ± 128	158.8 ± 17.1	0-11	—	—
Transition 2	14.54	584.8 ± 3.9	287 ± 112	164.7 ± 18.8	0-10	—	—
Bølling 2	14.42	624.4 ± 3.9	216 ± 109	178.5 ± 19.5	0-17	—	—
Bølling 1	14.42	621.1 ± 3.9	204 ± 111	177.9 ± 20.1	0-20	—	—
Allerød	13.00	647.2 ± 3.9	246 ± 90	190.2 ± 19.4	0-8	—	—
10.2K1	10.13	681.6 ± 3.9	126 ± 58	206.7 ± 20.7	0-11	32-56	131-168
10.2K2	10.13	681.6 ± 3.9	139 ± 57	206.7 ± 20.7	0-8	33-56	132-169
9.2K	9.21	659.7 ± 3.9	141 ± 63	200.4 ± 20.1	0-2	31-53	130-165
8.2K	7.94	623.9 ± 3.9	92 ± 74	187.8 ± 19.3	0-11	27-48	120-156
Late Holocene*	1.95	—	—	171.0 ± 18.8	0-9*	22-42	123-157

*The ¹⁴C-free emissions for this period are extrapolated from the average of ¹⁴C-free emissions in the early Holocene (10-8 ka BP). This assumption can be justified because a large change in the natural geologic emissions between the early Holocene and 2 ka BP seems unlikely, as global sea level and ice volume did not change significantly (36). We used both the stable isotopes (δ¹³CH₄, δD-CH₄) and CH₄ mole fraction from (11) at 2 ka BP to calculate the CH₄ bb and CH₄ mic emissions.